

## Activity of Cobalt Ions Dispersed in Magnesium Oxide for the Decomposition of Nitrous Oxide

A. CIMINO AND F. PEPE

*Istituto di Chimica Generale ed Inorganica, Università di Roma, Centro di Studio del C.N.R. su Struttura ed Attività Catalitica di Sistemi di Ossidi, Rome, Italy*

Received June 11, 1971

The catalytic decomposition of  $N_2O$  has been studied over CoO-MgO solid solutions (cobalt content from 0.05 to 50 atoms/100 Mg atoms), and over pure CoO. It has been shown that the activity per cobalt ion increases with dilution, and the apparent activation energy ranges from 17 kcal/mole on the most dilute solid solution to 29 kcal/mole on the most concentrated one and on pure CoO. Oxygen adsorption measurements taken during  $N_2O$  decomposition or obtained directly from molecular oxygen suggest the existence of at least two forms of adsorbed oxygen. Higher oxygen coverages are achieved when  $N_2O$  is decomposed; the result is discussed in terms of ionic interaction. The role of the matrix in oxygen desorption is examined: peroxy-ion formation is suggested as a possible mechanism. A comparison of the strength of the T-O<sub>ads</sub> bonds on CoO-MgO and NiO-MgO solid solutions (T = Co, Ni) is presented and discussed in terms of electronic configuration.

### I. INTRODUCTION

Earlier papers from this laboratory have reported the catalytic activity of systems made by dispersing nickel (1-3), chromium (4), and manganese (5) ions in oxides. This paper reports a study of the catalytic decomposition of  $N_2O$  by solid solutions of cobalt(II) oxide in magnesium oxide. The influence of the cobalt ion concentration and hence of the ionic interactions on the catalytic activity was thereby investigated. Chemical, structural (lattice parameter), magnetic, and spectroscopic (reflectance spectra) methods have been used to characterize the solid catalyst. Oxygen adsorption has also been measured to supplement the catalytic experiments.

### II. EXPERIMENTAL METHODS

#### *Catalyst Preparation and Chemical Analysis*

Catalysts were prepared by impregnation of magnesium oxide. Magnesium oxide

was prepared by thermal decomposition (600°C, 5 hr) of basic magnesium carbonate (reagent grade, Erba R.P.). The impregnation with a solution of cobalt nitrate was followed by drying at 100°C, firing at 600°C for 1 hr, regrinding, and finally firing at 1000°C for 5 hr. A portion of each specimen was further treated at 1200°C for 5 hr, and two specimens were treated at 1400°C. The samples are designated as MCo with number(s) after the letter giving the nominal cobalt atomic concentration per 100 magnesium atoms. The temperature of firing (°C) is given in parentheses. Pure CoO was obtained by thermal decomposition (600°C, 5 hr) of  $Co(NO_3)_2 \cdot 5H_2O$  (reagent grade, Erba R.P.) subsequent treatment at 1200°C for 5 hr and quenching (Q) in air. Further details of the preparation and analyses are described elsewhere (6). Table 1 lists the catalysts and their properties.

It was interesting to evaluate the rates of diffusion of cobalt ions in magnesium

TABLE 1  
 ANALYTICAL, X-RAY AND MAGNETIC DATA

Catalyst <sup>a</sup>	Cobalt content <sup>b</sup>	Lattice parameter (Å)	Magnetic data		Surface area (m <sup>2</sup> /g)	E <sub>a</sub> <sup>c</sup> (kcal/mole)
			μ (BM)	-θ (°K)		
MgO <sup>d</sup> (1000)	—	4.2116	—	—	19.0	36.0
MCo 0.05 (1000)	Not measured <sup>e</sup>	4.2116	—	—	13.0	19.2; 19.6
MCo 0.1 (1000)	Not measured <sup>e</sup>	4.2116	—	—	13.0	21.0; 22.0
MCo 1 (1000)	1.22	4.2120	5.30	32	7.6	21.0
MCo 5 (1000)	5.37	—	5.44	37	—	—
MCo 10 (1000)	10.4	4.2148	5.26	52	4.5	24.5
MCo 20 (1000)	18.2	4.221	5.20	65	1.9	—
MCo 50 (1000)	53.9	4.234	5.29	123	0.7	25.5
MCo 0.05 (1200)	Not measured <sup>e</sup>	4.2116	—	—	11.2	17.0
MCo 0.1 (1200)	Not measured <sup>e</sup>	4.2116	—	—	11.4	22.5; 21.0
MCo 1 (1200)	1.22	4.2124	5.33	20	14.0	22.5
MCo 5 (1200)	5.37	4.2142	5.32	48	2.3	—
MCo 10 (1200)	10.4	4.2168	5.33	20	4.3	22.0
MCo 20 (1200)	18.2	4.221	5.33	62	0.6	25.0; 22.5
MCo 50 (1200)	48.0	4.231	5.20	114	0.5	29.0
MCo 100 (1200)	92.5	4.238	5.30	155	0.4	—
CoO Q (1200)	—	—	—	—	0.2	29.5
MCo 0.1 (1400)	Not measured <sup>e</sup>	4.2120	—	—	3.7	29.5
MCo 50 (1400)	48.0	4.231	5.20	114	0.6	27
MCo 0.15 (s.c.) <sup>f</sup>	0.15	4.2117	—	—	0.77	27

<sup>a</sup> For key to designation of samples see text.

<sup>b</sup> Atoms per 100 Mg atoms.

<sup>c</sup> When two values are given for E<sub>a</sub>, they refer to independent sets of experiments.

<sup>d</sup> Value for pure MgO prepared at 1000°C ex carbonate.

<sup>e</sup> The concentration value has been considered as nominal in the normalized graphs.

<sup>f</sup> Single crystal obtained through the courtesy of Dr. F. S. Stone (Bristol).

oxide, and hence to estimate whether homogeneous solid solutions could be formed. The diffusion of Co<sup>2+</sup> ions in MgO has been studied by Wuensch and Vasilos (7, 8) and by Zaplatinsky (9). Even though they obtained somewhat different values for the diffusion parameters D<sub>0</sub> (diffusivity constant) and E (energy of activation), the diffusion coefficients D calculated at 1000°C and at 1200°C are not much affected by the choice of the diffusion parameters. For instance, taking the values from (9), D = 1.7 × 10<sup>-11</sup> at 1200°C, and from (7, 8), D = 0.41 × 10<sup>-11</sup> (cm<sup>2</sup> sec<sup>-1</sup>). Taking the values given by Zaplatinsky, and evaluating the depth of penetration x in time t by the formula KDt = x<sup>2</sup> (K, constant ~4), x is calculated to be 2.1 × 10<sup>-4</sup>

cm at 1000°C, and 1.1 × 10<sup>-3</sup> cm at 1200°C. Values of x of about one half of those quoted were obtained following Wuensch and Vasilos. It is apparent in both cases that the penetration depths are well in excess of the average diameter of the MgO particles, which can be evaluated by surface area methods to be of the order of 0.1 × 10<sup>-4</sup> cm. Therefore, the diffusion coefficients suggest that the rate of diffusion is sufficient to achieve complete penetration into the MgO particles.

#### X-Ray and Magnetic Analyses

The CoO-MgO system forms a continuous solid solution range (10-14). The lattice parameter a was measured with Mo-radiation for samples with low (<10%)

cobalt content, and with Fe-radiation for high ( $\geq 10\%$ ) cobalt content. The  $a$  values of the MCo 10 specimen, measured by both radiations, was found to be the same within the experimental errors. The error in  $a$  is larger when measured with Fe-radiation. The  $a$  values varied as expected ( $\theta$ ) and are reported in Table 1. A plot of  $a$  vs  $x_{Co}$ , where  $x_{Co}$  is the molar fraction of  $Co^{2+}$  ions, gives a good straight line (Fig. 1) for all MCo (1200) specimens. The MCo 10 (1000) and MCo 50 (1000) specimens show only fair agreement. The magnetic results conform to the behavior previously described ( $\theta$ ).

### Reflectance Spectra

Reflectance spectra of MCo specimens showed the characteristic absorption pattern of  $Co^{2+}$  ions in MgO (15, 15a, 16). The absorbance at 500 and 1200 nm increased linearly with  $x_{Co}$  for the MCo (1200) series, thus suggesting all the specimens were homogeneous. Specimens fired at  $1000^\circ$  of low ( $< 10\%$ ) cobalt content behaved similarly, while those of high co-

balt content, namely MCo 10 (1000) and MCo 50 (1000), showed an absorbance which was lower than expected. This result, together with the lattice parameter results, gives an indication that specimens with a high cobalt content are less homogeneous if fired at  $1000^\circ C$  only.

### Catalysis and Oxygen Adsorption Experiments

A static system was used [similar to the one previously described (1)] having a total volume of  $540\text{ cm}^3$ . The progress of the reaction with time was followed by condensing a small sample of the gaseous reactant mixture in a liquid nitrogen trap and measuring the pressure of the incondensable gas with a Pirani gauge. The reaction was followed up to a maximum of 1% decomposition of the initial  $N_2O$ . Pretreatment of 4 hr under vacuum at  $480^\circ C$  was applied to each fresh sample. Between runs, samples were conditioned *in vacuo* (at  $480^\circ C$ ) for 30 min. The pressure of the incondensable gas in the first experiment rose slowly at first, reaching a

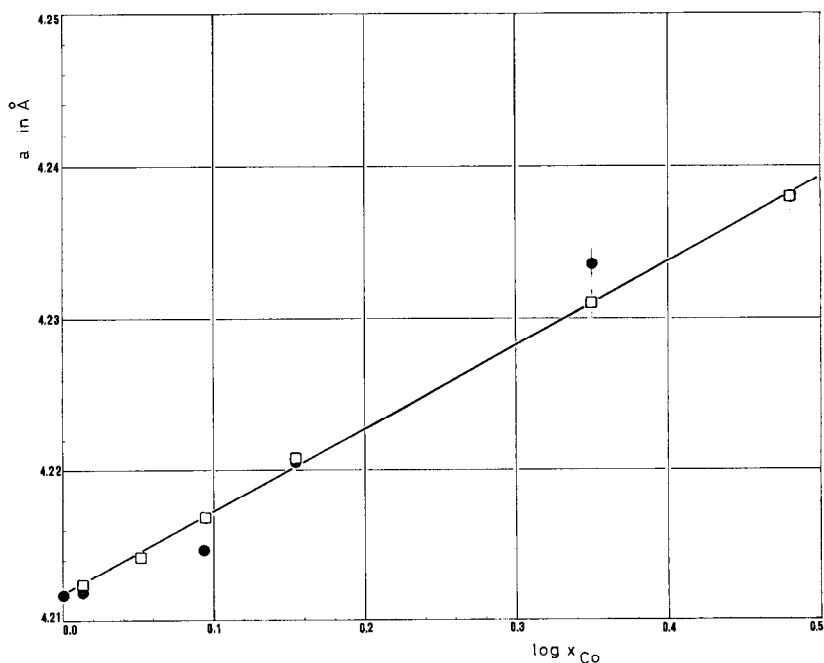


FIG. 1. Lattice parameter,  $a$ , vs cobalt molar fraction,  $x_{Co^{2+}}$ , for MCo samples: (□) fired at  $1200^\circ C$  for 5 hr; (●) fired at  $1000^\circ C$  for 5 hr.

linear dependence with time after only a few minutes; this time was dependent on the experimental temperature and it never exceeded 10 min. The nonlinearity of the initial part of the curve  $\Delta P$  vs  $t$ , is attributable to oxygen adsorption; succeeding runs showed a drastic reduction of the phenomenon, thus pointing to a reduced oxygen adsorption, as shown by the N<sub>2</sub>/O<sub>2</sub> ratios found in the first and succeeding experiments [Table 2, MCo 0.05 (1200)]. Calculation of the velocity constant was performed on the linear part of the  $\Delta P$  vs  $t$  curve, hence assuming a kinetic law

$$-\frac{dP_{N_2O}}{dt} = kP_{N_2O},$$

which is obeyed well for the small decomposition percentages investigated here. All data are reported as absolute velocity constants (cm min<sup>-1</sup>) (1).

Oxygen adsorption experiments were conducted in the same apparatus and with the procedure described by Cimino and Indovina (5). Briefly, fresh specimens underwent an outgassing treatment at 480°C

for 4 hr. Between adsorption runs, outgassing at 480°C for 30 min was adopted. Calculation of the amount of the more weakly bound oxygen (hereafter called "reversible oxygen") was obtained by measuring the amount of oxygen chemisorbed after outgassing for 30 min at the temperature of the preceding adsorption experiment (3, 5). Results on oxygen chemisorption during N<sub>2</sub>O decomposition were obtained by mass-spectrometric analysis of the N<sub>2</sub>/O<sub>2</sub> ratio of the gas, as previously described (1, 5).

### III. RESULTS

#### N<sub>2</sub>O Decomposition

The results are best illustrated by means of Arrhenius plots, which indicate immediately the reproducibility and the relative activities of the various catalysts. The reference line for MgO (Fig. 2) was taken from preceding work (1, 4, 5) and was further checked in the course of the present investigation. As already remarked (5),

TABLE 2  
OXYGEN CHEMISORPTION DURING N<sub>2</sub>O DECOMPOSITION

Catalyst <sup>a</sup>	Expt. <sup>b</sup>	<i>T</i> (°C)	<i>P</i> <sub>O<sub>2</sub></sub> <sup>c</sup> (Torr × 10 <sup>3</sup> )	N <sub>2</sub> /O <sub>2</sub>	Coverage <sup>d</sup> (θ × 100)
MCo 0.1 (1000)	c7	306	64	3.37	12.50
MCo 0.1 (1000)	c8	379	497	2.20	20.10
MCo 0.1 (1000)	c9	326	82	2.58	8.60
MCo 0.1 (1000)	c10	302	49	3.13	8.50
MCo 1 (1000)	a21	300	116	2.68	7.20
MCo 1 (1000)	a22	320	107	2.24	7.70
MCo 1 (1000)	a23	350	108	2.14	5.90
MCo 0.05 (1200)	b1	304	89	3.02	15.2
MCo 0.05 (1200)	b10	283	98	2.09	2.2
MCo 1 (1200)	a9	276	93	3.02	6.1
MCo 1 (1200)	a10	314	156	2.53	6.1
MCo 1 (1200)	a11	320	231	2.46	7.8
MCo 20 (1200)	a8	324	46	3.86	84.0
MCo 20 (1200)	a10	382	143	2.40	80.0
MCo 20 (1200)	a11	317	45	3.30	65.0

<sup>a</sup> For key to designation of samples see text.

<sup>b</sup> a, b, or c refers to a given portion of the catalyst, taken from a single batch; the numeral specifies the order of the experiment.

<sup>c</sup> Oxygen pressure calculated in absence of adsorption.

<sup>d</sup> Calculated for dissociative adsorption of oxygen per total number of cations as specified in Ref. (8).

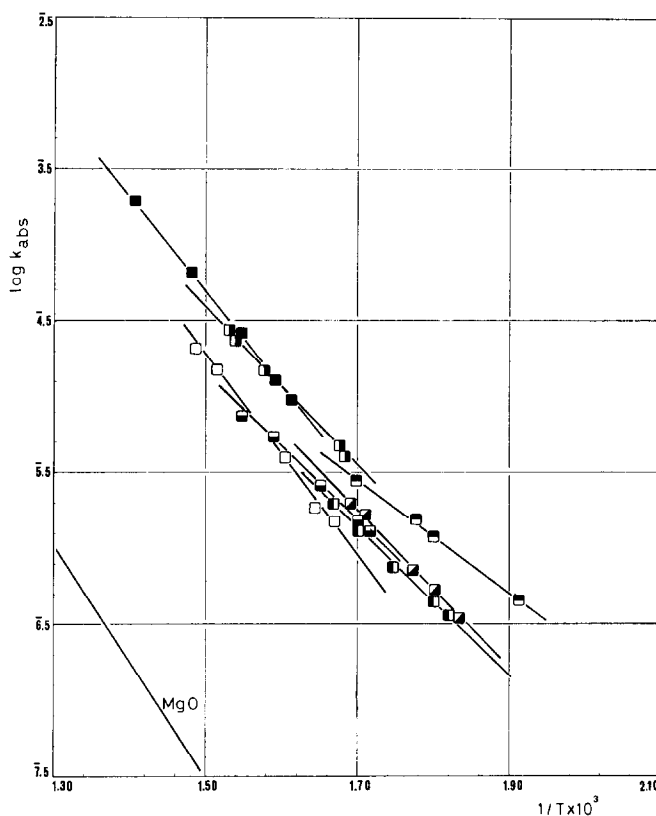


FIG. 2.  $\log k_{\text{abs}}$  vs  $1/T$  for MCo (1200) series: (■) MgO + 0.05% atomic CoO (MCo, 0.05); (▣) MgO + 0.1% atomic CoO (MCo 0.1); (□) MgO + 1% atomic CoO (MCo 1); (◻) MgO + 10% atomic CoO (MCo 10); (◻) MgO + 20% atomic CoO (MCo 20); (□) MgO + 50% atomic CoO (MCo 50); (■) CoO.

the absolute activity of pure MgO is highly reproducible. The reproducibility of the catalytic activity of different MCo specimens of equal composition was found to be satisfactory for all MCo (1200) specimens, and for MCo (1000) specimens of low cobalt content (scattering from 7 to 25% in  $k$  values). Specimens of the MCo (1000) series of high cobalt content (MCo 10, MCo 50) were less reproducible.

In order to illustrate the behavior of MgO-CoO solid solutions, the results obtained on the MCo (1200) series are reported in detail, as this series has been shown to meet all requirements of homogeneity. It is important to note, however, that the pattern is not altered if the series MCo (1000) is considered. In fact, the lower temperature series, as previously mentioned, can also be regarded as homog-

eneous if concentrations of cobalt below 10% are considered. Some data on solid solutions treated at temperatures higher than 1200°C are also reported.

**MCo (1200).** The increase of the catalytic activity brought about by additions of cobalt as small as 0.05 atomic % is remarkable (Fig. 2). A decrease in the apparent activation energy  $E_a$  with respect to pure MgO is also observed when small amounts of cobalt ions are introduced. In this respect, the MCo system behaves quite differently from those investigated before (2, 4, 5), which appeared to be less sensitive to small additions of the transition metal ions. Further additions of cobalt have comparatively little effect: a small variation in catalytic activity is observed. The position of pure CoO (1200) is also given in the same graph.

It should be noted that in passing from the very dilute MCo 0.05 specimen to the concentrated specimens, such as MCo 20 or MCo 50, the surface concentration of cobalt ions must vary greatly. The structural data which point to good homogeneity of the solid solutions, while not excluding *some* surface effect (such as some cobalt enrichment), are certainly against the possibility that no variation of cobalt concentration occurs in the surface concentration over the studied range of bulk concentrations. The fact that the absolute activities of all the catalysts are within a factor of 3 in the temperature range investigated, cannot therefore, be ascribed to a lack of variation in the surface concentration of cobalt over the whole series of catalysts. Therefore, a compensation effect must take place, which decreases the activity of potential centers as their number is increased. It is then instructive to

normalize the catalytic activity with respect to the number of cobalt ions, which, as specimen MCo 0.05 shows, are effective centers for the catalytic reaction. The result of the normalization is illustrated in Fig. 3, assuming that the surface molar fraction of cobalt is the same as the bulk molar fraction  $x_{Co}$ . The normalized plot of  $\log k_{abs}^{Co}$  vs  $1/T$  (where  $k_{abs}^{Co} = k_{abs}/x_{Co}$ ) shows that the activity per cobalt ion decreased continuously as the total cobalt concentration was increased.

**MCo (1000).** Specimens of this series are less active than the corresponding specimens with equal cobalt content fired at 1200°C. The low content specimens ( $\leq 10\%$  cobalt) show reproducible activity, while those of high concentration show limited reproducibility for different portions of the same batch. The general pattern is however the same, in particular: (i) the marked influence of as little as 0.05 Co

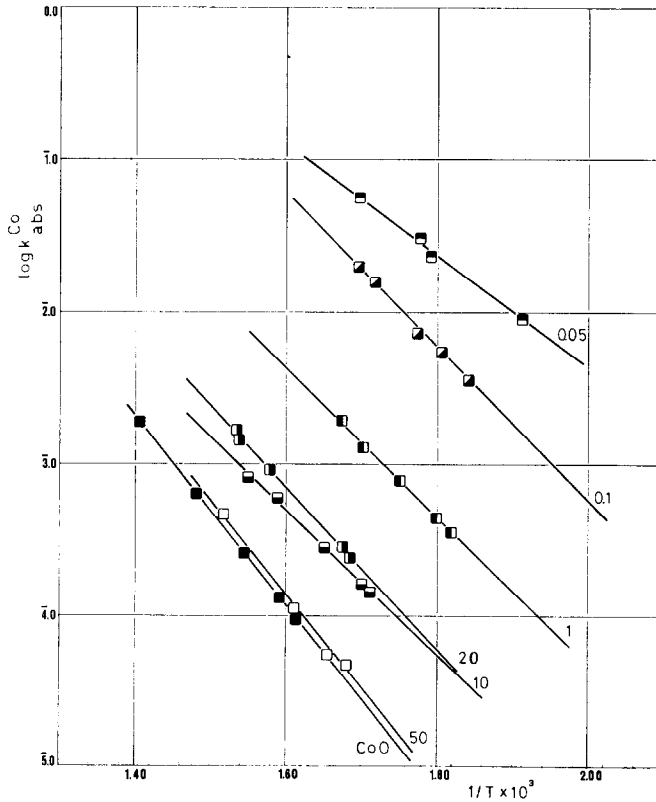


FIG. 3. Normalized activities ( $\log k_{abs}^{Co}$  vs  $1/T$ ) for MCo (1200).

atoms/100 Mg atoms on the catalytic activity; (ii) the grouping of absolute activities within factor of 2 for the whole concentration range from  $x_{\text{Co}} = 0.05 \times 10^{-2}$  (MCo 0.05) to  $x_{\text{Co}} = 0.33$  (MCo 50); (iii) a consistent decrease in activity per cobalt ion as the cobalt concentration is increased. The last statement is illustrated by Fig. 4, where a normalized Arrhenius plot for MCo (1000) specimens is shown, analogous to Fig. 3.

**Apparent activation energy.** The variation of the apparent activation energy  $E_a$  with cobalt content is illustrated in Fig. 5. The increase in  $E_a$  with increasing  $\text{Co}^{2+}$  concentration shows a trend similar to that found on NiO-MgO solid solutions (2). The increase in  $E_a$  appears to be stepwise for the MCo (1200) series. The data for MCo (1000) are not sufficient to show a clear pattern on their own, although they are not inconsistent with the results for the

MCo (1200) series. Concentration gradients and reproducibility errors which affect the result for the MCo (1000) series, render this series of less use in defining a clear pattern of the trend of  $E$  with Co.

**Decrease in activity per cobalt ion with increasing total concentration.** The decrease in activity per cobalt ion for both series (1000) and (1200) is illustrated in Fig. 6, which shows  $\log k_{\text{abs}}^{\text{Co}}$  vs  $\log x_{\text{Co}}$ , at two temperatures:  $270^\circ\text{C}$  ( $1/T = 1.8 \times 10^{-3}$ ) and  $350^\circ\text{C}$  ( $1/T = 1.6 \times 10^{-3}$ ). Note that if the catalytic activity of each cobalt ion was independent of the total cobalt concentration, a line parallel to the abscissa should be obtained. Figure 6 shows that a 10-fold increase in the total concentration causes approximately a 10-fold decrease in activity, with respect to each cobalt ion. It is also interesting to note that if the lower activity of the (1000) series with respect to the (1200) series is ascribed to

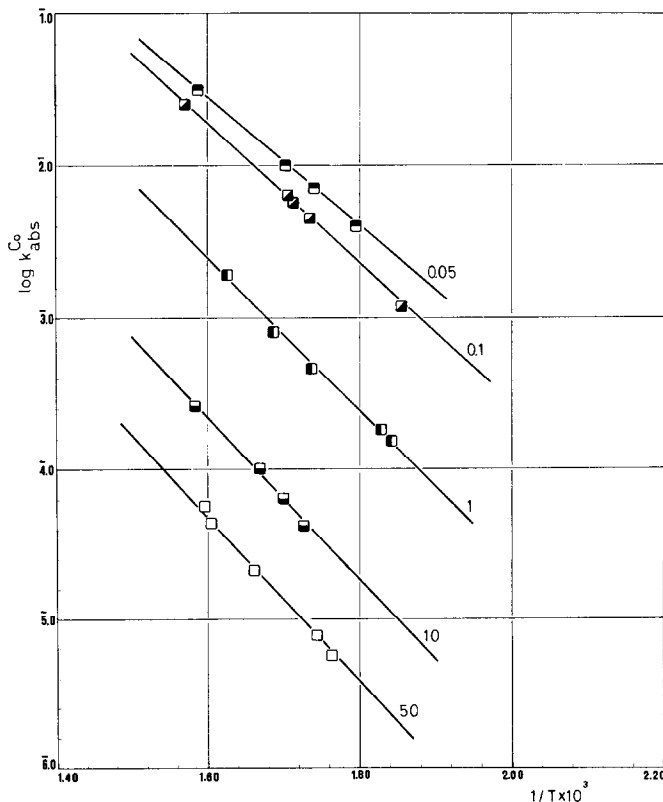


FIG. 4. Normalized activities ( $\log k_{\text{abs}}^{\text{Co}}$  vs  $1/T$ ) for MCo (1000).

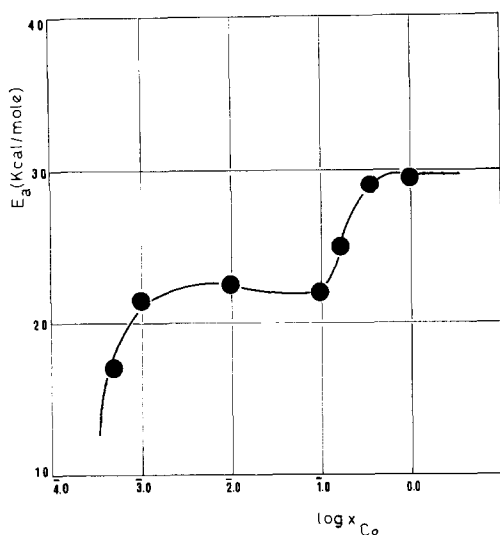


FIG. 5. Apparent activation energy,  $E_a$  vs cobalt molar fraction,  $x_{Co^{2+}}$ , for MCo (1200) samples.

greater effective surface concentration of cobalt in the former series than in the (1200) series, the dependence deduced from Fig. 6 would suggest an enrichment factor of about 3 between the surface concentration of series (1000) and (1200). This enrichment factor, even though not impossible, appears to be rather large in view of the small particle size of MgO, and the magnitude of the diffusion coefficient of Co<sup>2+</sup> in MgO (7, 8), which suggests that even at 1000°C the diffusion is complete, as previously shown. Further support for ascribing the difference in activity between the (1000) and (1200) series to factors other than surface enrichment in Co<sup>2+</sup> ions comes from the data on specimens fired at 1400°C (see below).

**MCo (1400).** The data for two specimens fired at 1400°C, MCo 0.1 and MCo

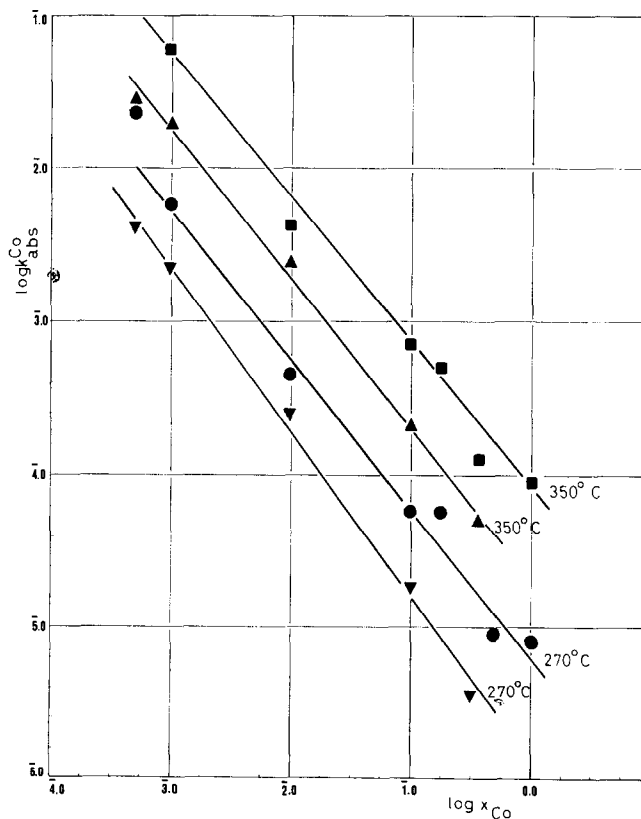


FIG. 6.  $\log_{abs} Co^{2+}$  (at 350 and 270°C) vs  $x_{Co^{2+}}$ : (■) MCo (1200); (▲) MCo (1000); (●) MCo (1200); (▼) MCo (1000).



50, are plotted in Fig. 7A and B. On the same graph, for comparison, the activity of the corresponding specimens fired at lower temperatures is reported. The initial activity of MCo 50 (1400) is considerably higher than the subsequent activity level reported in the graph. It is remarkable that in passing from a firing temperature of 1000 to 1200°C, the activity rises, while a firing at 1400°C depresses the catalytic activity. This observation is strongly opposed to the idea of segregation occurring in the outer layers, since the higher temperature should result in more homogeneous specimens, hence in more dilute surface solid solutions, and hence in higher activity. The fall in activity must evidently be ascribed

to other factors, related to high temperature effects on the structure of the solid surface.

**MCo—Single crystal.** A single crystal corresponding to an MCo 0.15 specimen was crushed, fired at 1200°C for 5 hr, and then tested for catalytic activity. Its Arrhenius plot is shown in Fig. 7A. As shown its activity is still lower than the MCo (1400) specimen. Since the preparation temperature of the single crystal (obtained by crystallization from bulk melt) was much higher than 1400°C, the decrease in activity with a firing temperature of above 1200°C is confirmed.

**Pure CoO.** The Arrhenius plot for pure CoO (Figs. 2 and 3) gives  $E_a = 29$  kcal/mole and an activity level between the

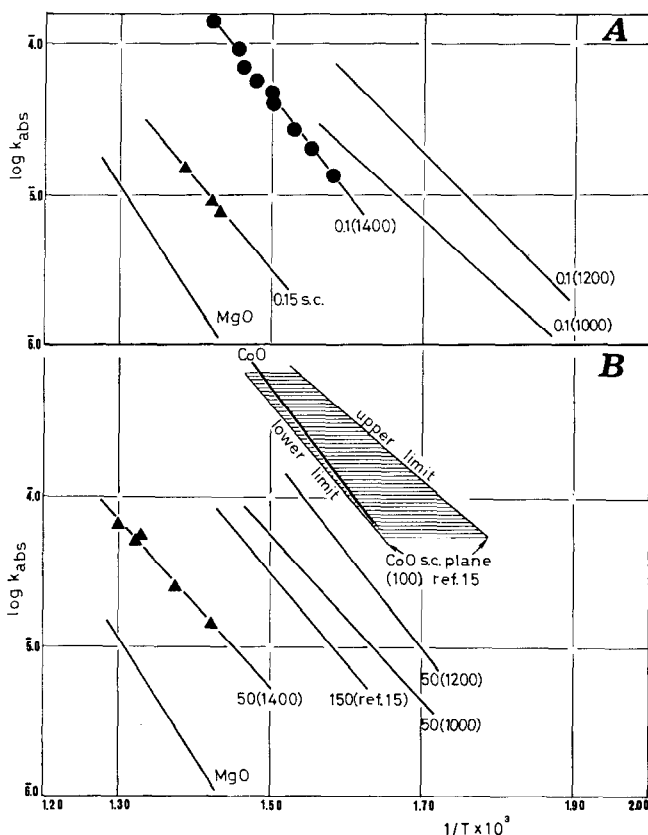


Fig. 7A.  $\log k_{abs}$  vs  $1/T$  for MCo 0.1 (1400) and MCo 0.15 single crystal (s.c.). Comparison of absolute activity level with MCo 0.1 (1200) (from Fig. 2) and MCo 0.1 (1000) (from Fig. 4). (B)  $\log k_{abs}$  vs  $1/T$  for MCo 50 (1400); comparison of absolute activity level with MCo 50 (1200) (from Fig. 2); MCo 50 (1000) (from Fig. 4); and MCo 150 (s.c.) [Ref. (15)]. Comparison of absolute activity level of CoO powder (from Fig. 2) with CoO (s.c.) (100) plane [Ref. (15)].

two extremes given by Volpe and Reddy (17) for the (100) plane of a single crystal (see Fig. 7B).

#### Oxygen Chemisorption During Catalysis

Illustrative examples of data referring to catalysts submitted to a succession of N<sub>2</sub>O decomposition experiments are reported in Table 2, where the sequence in which the experiments were done is specified by the run number. It was found that the amount of oxygen chemisorbed at a given temperature in the initial experiment was larger, but it rapidly decayed in succeeding runs as clearly shown by MCo 20 and MCo 0.05 in Table 3.

Because of the large errors involved and of the limited number of experiments for each catalyst, it is possible to assess the dependence of coverage upon catalyst composition in a qualitative way only. It is clear, however, that the oxygen coverage is increased by the addition of cobalt ions to pure magnesium oxide. In fact, while pure MgO shows a coverage of 0.4% at 400°C (1), specimens prepared at 1200°C and containing 0.05 or 1 cobalt atom/100 Mg atoms show an oxygen coverage of 2.2% (283°C), and 7.8% (320°C), respectively. Furthermore, as shown, there is little increase in oxygen coverage in passing from an MCo 0.05 ( $\theta = 2.2\%$ ) to an MCo 1 specimen ( $\theta = 6.1\%$ ), in comparison to the increase found on passing from MCo 1 ( $\theta = 6.1\%$ ) to MCo 20 ( $\theta = 65.0\%$ ), i.e., for the same increase in cobalt concentration. A final observation is that coverage values are larger than those observed in analogous experiments carried out on NiO-MgO solid solutions (1).

#### Chemisorption from Molecular Oxygen

The data are reported in Table 3, which lists the "total" and the "reversible" oxygen uptake (percentage coverages). The data are listed in the same order in which they were taken; the latter r refers to the determination of the "reversible" oxygen. As shown:

a. The first adsorption experiments on a fresh catalyst, outgassed at 480°C for 4 hr, indicates oxygen coverage values notice-

TABLE 3  
OXYGEN CHEMISORPTION FROM  
MOLECULAR OXYGEN

Run <sup>a</sup>	T (°C)	P <sub>O<sub>2</sub></sub> (Torr × 10 <sup>3</sup> )	$\theta_{30}^b$ (%)	$\theta_{\infty}^b$ (%)	t <sup>c</sup> (min)
MCo 0.1 B					
1	367	436	2.2	3.7	120
1r	367	360	0.9	1.9	870
2	288	432	—	—	140
3	318	408	—	—	120
4	330	370	1.1	2.1	345
4r	330	367	—	1.5	886
5	317	83	0.4	0.7	140
6	300	109	1.1	2.6	270
6r	300	104	0.3	0.4	66
7	278	92	0.7	0.8	91
7r	278	88	0.2	0.3	120
MCo 1 B					
1	302	178	4.5	5.8	68
1r	300	199	0.9	0.9	30
2	320	205	1.3	1.4	36
2r	320	196	0.5	0.6	49
3	300	171	0.6	0.9	140
3r	300	182	—	—	40
4	276	187	—	—	40
4r	276	199	—	—	40
5	330	184	0.4	1.0	174
5r	330	200	—	—	40
MCo 20 B					
1	326	128	88.6	100	62
1r	326	60	19.2	19.4	49
2	382	114	14.0	14.0	30
2r	382	93	6.1	6.1	30
3	330	80	8.4	8.4	30
3r	330	66	2.6	4.5	65
4	382	156	8.0	20.0	237
4r	382	157	1.4	1.4	47
5	326	72	3.7	3.7	30
5r	326	100	2.6	3.8	57
6	384	137	5.8	17.0	259
6r	384	104	2.2	2.2	63
7	332	54	3.2	4.1	63
7r	332	79	1.7	4.3	164
8	376	138	6.1	7.1	85
8r	376	111	2.1	2.1	60

<sup>a</sup> The run number specifies the order in which the experiment was taken for each given specimen; r = "reversible" oxygen (see text).

<sup>b</sup> Coverages (%) calculated for dissociative oxygen adsorption per total number of cations as specified in the text:  $\theta_{30}$  refers to coverages measured after 30 min; and  $\theta_{\infty}$  to pseudo-equilibrium (see text).

<sup>c</sup> Time (min) required to reach  $\theta_{\infty}$ .

ably larger than those observed in succeeding adsorption experiments. The decrease of coverage with increasing number of experiments continues, but in a less marked manner.

b. Oxygen coverages are considerably lower than those observed during  $N_2O$  decomposition.

c. The dilute solid solutions (MCo 0.1, MCo 1) behave differently from the concentrated one (MCo 20) with respect to the initial oxygen uptake. In fact, while it is possible to reach 100% oxygen coverage on MCo 20, the coverage on MCo 1 reaches a value of the order of 6% only.

d. The decrease of oxygen coverage from the initial to the stationary condition is very pronounced for MCo 20, since the coverage at about  $330^\circ C$  goes from  $\theta = 100\%$  (run 1) to  $\theta \simeq 4\%$  (runs 5 and 7). For MCo 0.1 or MCo 1, stationary level values are not available, but, as shown, after the same number of experiments (five) the coverage values have decreased less markedly.

e. An important parameter is the time of adsorption. Table 3 gives oxygen coverages after 30 min ( $\theta_{30}$ ) and "pseudo-equilibrium" coverages ( $\theta_\infty$ ), defined as those values which are not changed in three successive readings at 10 min intervals. The time necessary to reach  $\theta_\infty$  is given in the last column. This time is longer for the dilute specimen MCo 0.1, than for MCo 1 or MCo 20. Furthermore, if the time of adsorption is prolonged, as in experiments MCo 0.1 (run 1 or 4), subsequent experiments indicate little (run 5) or no adsorption (run 2) and little or no reversible oxygen, thus pointing to the existence of a strong form of adsorbed oxygen, created in the long runs 1 and 4. The strong form is removed with difficulty in the next experiment. Similar behavior is found with catalyst MCo 1 (runs 3 and 5) and (though less pronounced) for catalyst MCo 20 (runs 4 and 6). It can be argued that on all catalysts a transformation can take place from weakly held oxygen to a more strongly held form. The long times needed to achieve a strongly held form in the case of MCo 0.1, together

with the shorter times sufficient for catalyst MCo 20, and with the fast decay of adsorption (point d), suggest that the transformation from a weak to a strongly held form is slower on MCo 0.1 than on MCo 20.

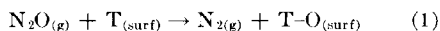
#### IV. DISCUSSION

Cobalt oxide is known (18-21) to be a very active catalyst for  $N_2O$  decomposition. The present results prove that cobalt ions are very active also when dispersed in the magnesium oxide matrix. The catalytic activity per cobalt ion increases as dilution is increased (Figs. 3, 4), thus confirming a trend established for other transitional metal ions. When a transition metal ion  $M^{n+}$  is dispersed in the MgO matrix, interactions can occur between  $M^{n+}$  ions which are found to be active centers for  $N_2O$  decomposition, and only in "dilute" systems can these be safely neglected. However, the actual concentration range which can be defined as "dilute" depends upon the species  $M^{n+}$ . Thus, while for nickel ions in MgO, a 1% and a 0.5% dilution gives equal activities per nickel ion, in the case of cobalt there is a marked fall in catalytic activity on passing from 0.05 to 0.1%. Hence, for cobalt, even a 0.1% solution cannot be considered as dilute. The reduction of intrinsic activity caused by an increase of concentration appears to be more severe for the more active centers  $Co^{2+}$  than for  $Ni^{2+}$ . An increase in the  $E_a$  value accompanies the decrease in activity as the cobalt ion concentration is increased. Remembering that previous work on transition metal oxides in solid solution has pointed out the importance of the surface oxygen complex (2-5, 31), the change of activity per cobalt ion with dilution and the apparently discontinuous variation of  $E_a$  point to a change in the nature of the surface oxygen complex as the  $Co^{2+}$  concentration is varied. Some aspects regarding the oxygen-surface interaction, relevant to  $N_2O$  decomposition, are therefore discussed first. Subsequently, the influence of the temperature of preparation, and of the state of the surface in solid solutions and in pure oxides are examined.

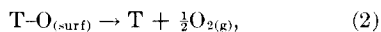
**Oxygen chemisorption and catalysis.** A remarkable feature of the CoO–MgO solid solution is the high oxygen coverage attained during the catalytic decomposition of N<sub>2</sub>O. Let us compare the NiO–MgO system (1, 2) with the present one to illustrate this feature. For particular extents of N<sub>2</sub>O decomposition (dec %), giving the coverage  $\theta\%$  as a percentage value of the monolayer capacity (1), we have:

	Dec (%)	$\theta$ (%)
MN 1 (350°C)	0.14	0.41
MCo 1 (320°C)	0.77	7.8

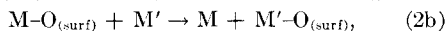
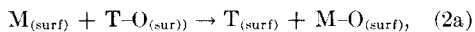
It is believed that this fact points to participation of the matrix in the N<sub>2</sub>O decomposition process; that is, the oxygen left by the decomposed N<sub>2</sub>O molecules does not simply desorb from the center which is active for the decomposition, but the oxygen can migrate *via* the matrix surface and desorb. The transition metal ion T is therefore active in carrying out the decomposition step, such as



(electron transfer is not shown), but the succeeding step, such as



takes place with the intermediate participation of the matrix, and reaction (2) should be replaced schematically by (M, M' = matrix sites):



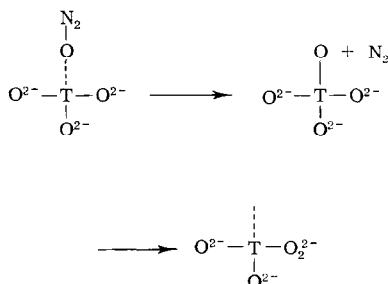
(Once again, no electrons are shown for simplicity.) A high catalytic activity of a transition metal ion in solid solution is therefore not simply linked to a favorable activity for reaction (1), but it must also involve a fast step (2a), which is not dependent solely on the T–O bond strength but also on the capacity of the matrix to favor the oxygen accommodation, followed by migration and desorption.

Before commenting further on the N<sub>2</sub>O decomposition steps, it is relevant to examine the behavior of CoO–MgO solid solutions towards oxygen adsorption from

molecular oxygen. The data of Table 3 show that there is a large initial capacity for adsorption from molecular oxygen, and a subsequent fall of this capacity. The initial capacity can derive from the fact that the originally prepared MgO surface is hydroxylated, and that the conditioning in vacuum at 480°C gives rise to bare sites, likely to chemisorb oxygen strongly. The fall in the oxygen adsorption capacity shown in successive experiments is then caused by the impossibility of regeneration of the same surface. It is noticeable that even in the case of molecular oxygen, the ensuing oxygen coverage must involve part of the matrix surface, at least in the initial experiments. It is also noteworthy that *dilute* specimens require a *longer* time for reaching their  $\theta_\infty$  values in comparison to concentrated specimens. An additional observation is that after long adsorption times, the amount of desorbable oxygen is greatly reduced. It can be deduced that, as time progresses, a transformation takes place from a weakly held form of oxygen to a strongly held one. This transformation is more rapid with concentrated specimens as pointed out in paragraph (e) above. This observation can be rationalized if multiple centers such as ion pairs Co<sup>2+</sup> . . . Co<sup>2+</sup> play a significant role in achieving the strongly adsorbed form. In fact, a cobalt ion pair may be essential in order to break the O–O bond of the O<sub>2</sub> molecule. The occurrence of such pairs is less likely for dilute specimens.

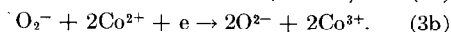
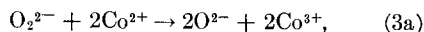
The oxygen adsorption from molecular oxygen and that occurring during catalysis can now be compared. During the N<sub>2</sub>O decomposition, the amounts of oxygen adsorbed (and therefore the amounts of oxygen desorbed during evacuation between runs) are larger than those found for the adsorption from molecular oxygen, even after the surface has been subjected to several runs. However, initial capacities are not very different (see Tables 2 and 3). This suggests that the N<sub>2</sub>O decomposition sustains a weak form of adsorbed oxygen, which can be reversibly eliminated by outgassing between N<sub>2</sub>O decomposition experiments.

Coming back to the hypothesis that  $N_2O$  decomposition takes place through steps such as (2a), (2b), and (2c) involving oxygen migration along the matrix surface, the type of surface complex responsible for the migration should be considered. It has been suggested that the formation of a peroxide ion may be involved at this stage (22, 23) according to the following scheme:



followed by migration of oxygen atoms along the surface ( $O_2^{2-} + O^{2-} \rightarrow O^{2-} + O_2^{2-}$ ) until an oxygen molecule is desorbed, either from two peroxide ions, or from a peroxide and an oxide ion, when favorable conditions can be found for the creation of an anion vacancy (for instance, at edges). It is not necessarily required that the weak oxygen form originating from the  $N_2O$  decomposition is the same weak form originating from the adsorption of molecular oxygen. There may be a difference in the origin of the weak form: the one coming from decomposed  $N_2O$ , i.e., from oxygen atoms, is of the form  $O_2^{2-}$  (peroxyions), and can lead to high oxygen coverages if the matrix lends itself, as the MgO matrix does, to peroxy-formation; the one coming from molecular oxygen could be of the form  $O_2^-$  (superoxy-) and it is less likely to lead to high coverages. The  $O_2^-$  species has been identified at 110°C over MgO by Tench and Lawson (24); thus it is a plausible intermediate even at somewhat higher temperatures. However, both in  $N_2O$  decomposition and oxygen adsorption an increase in cobalt content favors a shift towards the strong form of oxygen adsorption. The strong form must be atomic in character, and the  $O^{2-}$  form is the most plausible one, since the temperatures at which the strong form is desorbed

are close to the temperatures where decomposition of the higher oxide ( $Co_3O_4$ ) begins (25-27). The transformations could be schematically represented by:



The two equations justify the suggestion that the weak form changes to the strong one as the cobalt ion concentration is increased. As a result of the formation of strongly held oxygen in concentrated cobalt solid solutions, the catalytic activity for  $N_2O$  decomposition decreases; while in oxygen adsorption experiments, a marked fall (%) of the oxygen adsorption capacities is observed. The shift from weak to strong form is therefore likely to be an activated process, favored by concentrated solid solutions.

**Solid solutions and pure oxides.** Concentrated solid solutions will tend to resemble pure transition metal oxides, provided that the pure oxide does not show a surface defective structure widely different from the one existing in the concentrated solid solution. If a concentrated specimen such as MCo 50 is considered, in spite of the insertion of a considerable number of  $Mg^{2+}$  ions between the  $Co^{2+}$  ions the local situation is not dissimilar from that found in pure CoO, since many extended  $Co^{2+} \cdots O \cdots Co^{2+} \cdots$  domains can be found, i.e., conditions similar to pure CoO. Thus, MCo 50 has an  $E_a$  value equal to that of pure CoO (29 kcal/mole), and a catalytic activity per cobalt ion which is also comparable to that shown by pure CoO (Fig. 6). The similarity between MCo 50 and pure CoO also helps in a comparison of the results obtained on pure cobalt oxide by different authors. The cobalt oxide used in earlier decomposition experiments (18, 19) had not been subjected to treatment at high temperatures. At low temperatures, the higher oxide  $Co_3O_4$  is formed (27). According to Bielanski and co-workers (28), treatment at high temperature ( $\geq 1200^\circ C$ ) is capable of removing the excess oxygen. It is true that the thermodynamic stability of  $Co_3O_4$  at lower temperatures will favor formation to  $Co_3O_4$

as the lower range of temperature is crossed during the quenching of the specimen in air. However, if the higher oxide is formed on the surface only, as suggested by the slowness of the transformation  $\text{CoO} \rightarrow \text{Co}_3\text{O}_4$  (26), outgassing at about 500°C will be enough to reestablish the CoO stoichiometry (25). Behavior actually attributable to the oxide CoO can then be expected only when oxides treated at high temperatures ( $\geq 1200^\circ$ ) are investigated, such as our CoO specimens, or single crystals formed at high temperatures (17). A cobalt-rich solid solution in MgO, on the other hand, is necessarily similar to the CoO oxide because of the stabilization of the +2 oxidation state in the MgO structure (29). This explains why a similarity can be found between CoO–MgO solid solutions and our CoO specimens (the CoO single crystals, as is discussed below, also behave similarly) but not between our CoO specimens and the low-temperature-prepared CoO specimens of earlier investigators.

**Effect of calcining temperature.** The (1200) specimens showed the highest activity. The increase in activity on passing from (1000) to (1200) series could be explained by a more homogeneous distribution of Co<sup>2+</sup> ions, the ions becoming less concentrated near the surface, thus leading to a higher activity per cobalt ion because of the dilution effect. In other words, the dilution outbalances the effect of the decrease in the number of Co<sup>2+</sup> ions per unit area. However, the decrease in activity found when treatment at 1400°C is carried out, calls for a different explanation. It is believed that the decrease in activity with high firing temperature is linked to the participation of the matrix. The high temperature material has a more ordered structure, and the matrix is less apt to intervene in the secondary steps (2b) and (2c) of oxygen diffusion along the surface and oxygen desorption. The decrease in the ability of the matrix to participate in the oxygen transfer process is likely to be continuous from 1000 to 1400°C. However, the activity of Co<sup>2+</sup> in the primary step ( $\text{N}_2\text{O} \rightarrow \text{N}_2 + \text{O}_{\text{ads}}$ ) increases at first, until a

homogeneous solid solution is achieved, as discussed before. The two factors (the one due to the cobalt ion efficiency, and the one due to a matrix effect), which have opposing trends with increasing temperature, can give rise to a maximum in the activity at 1200°C. The importance of the role of the matrix arose independently from studies of N<sub>2</sub>O decomposition with other oxide systems (ZnO, Ni–Al<sub>2</sub>O<sub>3</sub>, MgAl<sub>2</sub>O<sub>4</sub>) (30–32).

**Comparison with single crystal work.** A comparison of catalytic activity of CoO and MCo solid solution (powders) with single crystal work (17) must consider two factors: (a) the different conditions in the formation of single crystal material with respect to powders; (b) the very large difference in surface areas and surface topography. It is interesting that in spite of the different conditioning carried out by Volpe and Reddy (17), and of the variability of activity found by these authors, the absolute activities [absolute velocity constants ( $\text{cm min}^{-1}$ )] match reasonably well, especially if the large factor ( $\sim 100$ ) of surface areas is considered. The agreement is good for pure CoO (our sample falls within the two extremes determined by Volpe and Reddy). Volpe and Reddy's MCo 60/40 single crystal, corresponding to MCo 150 in our nomenclature, is less active by a factor of about 7. Such a difference can be accounted for by the higher preparation temperature of the single crystal specimen. Our (1400) samples are less active than the (1200) ones. The very high temperature involved in the formation of single crystals can explain a further decrease in activity per unit surface area, when the single crystal is considered. Furthermore, the different conditioning adopted in the two cases can also introduce some divergence.

**Comparison between cobalt and nickel oxides and related solid solutions.** In both cases, pure oxides and solid solutions in MgO, cobalt ions are more active than nickel ions for N<sub>2</sub>O decomposition. The activity of numerous oxides has been successfully related by Winter (33, 34) to their ability to act as a catalyst for homomolecular exchange and hence related to

the lability of the metal-oxygen bond. Data on the homomolecular exchange for both NiO and Co<sub>3</sub>O<sub>4</sub>, which is the oxide formed on the surface of CoO when N<sub>2</sub>O is decomposed on it (35), are given by Boreskov (36), and it can be seen that the same trend is obeyed, since Co<sub>3</sub>O<sub>4</sub> is more active than NiO for the homomolecular exchange reaction. In considering solid solutions of transition metal oxides in inert oxides it is necessary to distinguish cases when the matrix is able to carry out reactions (2a), (2b), and (2c), as MgO is, from those such as ZnO where the matrix can limit the catalytic activity of ions (31). Here we are concerned with a matrix, MgO, which does not prevent the cobalt ions reaching their high catalytic activity. Hence we can discuss the catalytic activity shown by two different ions, Co<sup>2+</sup> and Ni<sup>2+</sup>, dispersed in MgO, by focusing attention on the oxygen loss reaction from the transition metal ion to the matrix (2a). The kinetic data on NiO-MgO solid solutions (37) clearly show the retarding effect of oxygen. Furthermore, for both NiO and CoO in solid solution in MgO, there is a decrease in activity per metal ion as the concentration is increased, which is attributed to the transformation of the oxygen surface complex into a strong form, assisted by the easier electron transfer. This decrease can be regarded, without a change of view on the discrete nature of the process, as proof that oxygen retards the N<sub>2</sub>O decomposition. Step (2a) is therefore critical. Both the high catalytic activity and the high oxygen coverage found for CoO-MgO specimens show that reaction (2a) is faster on CoO-MgO than on NiO-MgO. It thus appears that the T-O<sub>ads</sub> bond is weaker for Co<sup>2+</sup> than for Ni<sup>2+</sup>. It is interesting to note that this result is correctly predicted by a crystal field stabilization energy (CFSE) approach, which establishes that restoration of full octahedral symmetry (by O adsorption) is accompanied by a larger gain in energy for Ni<sup>2+</sup> than for Co<sup>2+</sup> (38, 39).

#### ACKNOWLEDGMENTS

The authors thank Dr. F. S. Stone for valuable discussion and for critically reading the

manuscript, and Mr. G. Minelli, for technical assistance in the characterization of the specimens. The partial financial support of the NATO Scientific Programme is gratefully acknowledged.

#### REFERENCES

1. CIMINO, A., BOSCO, R., INDOVINA, V., AND SCHIAVELLO, M., *J. Catal.* **5**, 271 (1966).
2. CIMINO, A., INDOVINA, V., PEPE, F., AND SCHIAVELLO, M., *J. Catal.* **14**, 49 (1969).
3. CIMINO, A., SCHIAVELLO, M., AND STONE, F. S., *Discuss. Faraday Soc.* **41**, 350 (1966).
4. CIMINO, A., INDOVINA, V., PEPE, F., AND SCHIAVELLO, M., *4th Int. Congr. Catal., Moscow, 1968*, Pap. No. 12.
5. CIMINO, A., AND INDOVINA, V., *J. Catal.* **17**, 54 (1970).
6. CIMINO, A., LO JACONO, M., PORTA, P., AND VALIGI, M., *Z. Phys. Chem. Neue Folge* **70**, 166 (1970).
7. WUENSCH, B. J., AND VASILOS, T., *Nat. Bur. Stand. (U. S.), Spec. Publ.* **n296**, 95 (1967).
8. WUENSCH, B. J., AND VASILOS, T., *J. Chem. Phys.* **36**, 2917 (1962).
9. ZAPLATINSKY, I., *J. Amer. Ceram. Soc.* **45**, 28-31 (1962).
10. ROBIN, J., AND PASCAL, P., *C. R. Acad. Sci.* **1301**, 1959.
11. ZINTL, G., *Z. Phys. Chem. Neue Folge* **48**, 340 (1965).
12. ELLIOTT, N., *J. Chem. Phys.* **22**, 1924 (1954).
13. PERAKIS, N., AND SERRAS, A., *J. Phys. Radium* **18**, 47 (1957).
14. COSSEE, P., *Mol. Phys.* **3**, 125 (1960).
15. LOW, W., *Phys. Rev.* **109**, 256 (1958).
- 15a. REINEN, D., *Mh. Chem.* **96**, 730 (1965).
16. PAPPALARDO, R., WOOD, D., AND LINARES, R. C., JR., *J. Chem. Phys.* **35**, 2041 (1961).
17. VOLPE, M. L., AND REDDY, J. F., *J. Catal.* **7**, 76 (1967).
18. STONE, F. S., RUDHAM, R., AND GALE, R. L., *Z. Elektrochem.* **63**, 129 (1959).
19. SCHMID, G., AND KELLER, N., *Naturwissenschaften* **37**, 43 (1950).
20. AMPHLETT, C. B., *Trans. Faraday Soc.* **50**, 273 (1954).
21. DELL, R. M., STONE, F. S., AND TILEY, P. F., *Trans. Faraday Soc.* **49**, 201 (1953).
22. BICKLEY, R. I., AND STONE, F. S., *Trans. Faraday Soc.* **64**, 3393 (1968).
23. DOWDEN, D. A., *Catal. Rev.* **5**, 1 (1971).
24. TENCH, A. J., AND LAWSON, T., *Chem. Phys. Lett.* **7**, 459 (1970).
25. GULBRANSEN, E. A., AND ANDREW, K. F., *J. Electrochem. Soc.* **89**, 241 (1951).
26. O'BRIAN, H. M., AND PARRAVANO, G., *Reactivity of Solids 5th Intern. Symposium Munich 1964*, p. 256, Elsevier, Amsterdam, 1965.

27. ROBIN, J., *Ann. Chim.* [s12] **10** (1955).
28. BIELANSKI, J., DYREK, K., NIZIOL, S., AND ROMANOWKA, T., *Bull. Acad. Pol. Sci.* **15**, (12) (1967).
29. TIKKANEN, M. H., ROSSELL, B. O., AND WIBERG, O., *Acta Chem. Scand.* **17**, 513 (1963).
30. CIMINO, A., AND SCHIAVELLO, M., *J. Catal.* **20**, 202 (1971).
31. SCHIAVELLO, M., CRIADO, J. M., CIMINO, A., *Gazz. Chim. Ital.* **101**, 47 (1971).
32. SCHIAVELLO, M., LO JACONO, M., CIMINO, A., *J. Phys. Chem.* **75**, 1051 (1971).
33. WINTER, E. R. S., *J. Chem. Soc. (A)* **1968**, 2889-2902.
34. WINTER, E. R. S., *Discuss. Faraday Soc.* **28**, 183, 1959.
35. MATSUURA, I., KUBAKOWA, Y., AND TOYAMA, O., *Nippon Kagaku Zasshi* **81**, 1205 (1960).
36. BORESKOV, G. K., "Advances in Catalysis and Related Subjects" (D. D. Eley, H. Pines, and P. B. Weisz, eds.), Vol. 15, p. 285. Academic Press, New York, 1964.
37. CIMINO, A., INDOVINA, V., PEPE, F., AND STONE, F. S., unpublished data.
38. BASOLO, F., AND PEARSON, R. G., "Mechanisms of Inorganic Reactions" 2nd ed. p. 146. Wiley, New York, 1967.
39. KLIER, K., *J. Catal.* **8**, 14 (1967).